ELSEVIER

Scopus

doi

Journal of Vibration Engineering

ISSN:1004-4523

Registered

- SCOPUS
- GOOGLE SCHOLAR
- DIGITAL OBJECT IDENTIFIER (DOI)
- IMPACT FACTOR 6.1

Our Website
www.jove.science

Seasonal and Diurnal Variations of Precipitation and Rain Attenuation over 5G Communication Links in Johannesburg, South Africa

O. A. Layioye[1*], P. A. Owolawi[2], C. Tu[3], and J. S. Ojo[4]

[1,2,3]*Department of Computer Systems Engineering, Faculty of Information and Communication Technology, Tshwane University of Technology, Pretoria 0152, South Africa*

[4]*Department of Physics, The Federal University of Technology Akure 340110, Nigeria*

ORCID: 0009-0003-7243-5994

Abstract: *The deployment of fifth-generation (5G) networks, particularly in millimeter-wave (mmWave) bands, is significantly challenged by rain-induced signal attenuation, especially in regions with convective rainfall patterns. This study presents a comprehensive six-year (2010–2015) analysis of rain attenuation characteristics for 5G Frequency Range 1 (FR1: 3.5 GHz) and Frequency Range 2 (FR2: 30 GHz) in Johannesburg, South Africa. Using high-resolution hourly precipitation data and ITU-R models, we quantify attenuation, analyze its statistical properties, and characterize its temporal variations. Results reveal attenuation at 30 GHz is approximately 1,600–1,750 times greater than at 3.5 GHz, with maximum values exceeding 37.5 dB for a 7 km path during summer. Statistical analysis shows highly right-skewed, leptokurtic distributions, dominated by dry periods but punctuated by intense, short-duration events. Pronounced seasonal peaks occur in summer (December to February: DJF) and spring (September to November: SON), with a distinct diurnal peak in the late afternoon to early evening. These findings underscore the severe vulnerability of mmWave links to rain fade and provide essential data for designing robust fade margins, adaptive network strategies, and informed spectrum allocation for reliable 5G and beyond-5G wireless services in subtropical urban environments.*

Keywords: Rain attenuation, 5G networks, Millimeter-wave (mmWave), Fade margin, Mie-scattering, 5G Frequency range 1 (FR1) and 2 (FR2), Subtropical highland climate.

1. Introduction

The global telecommunications landscape is undergoing a paradigm shift with the deployment of fifth-generation (5G) networks, promising unprecedented data rates, ultra-low latency, and massive device connectivity [1]. However, this technological advancement brings forth significant propagation challenges, particularly in the context of millimeter-wave (mmWave) frequencies allocated for 5G's high-frequency bands [2]. Among these challenges, rain attenuation emerges as a critical limiting factor that can severely degrade signal quality and network reliability, especially in tropical and sub-tropical regions characterized by intense convective rainfall [3].

Rain attenuation represents the scattering and absorption of radio waves by rain droplets along the propagation path, with severity increasing exponentially with frequency [4]. While traditional sub-6 GHz networks experience moderate rain-induced signal degradation, the 5G mmWave bands (24-52 GHz) are particularly vulnerable, with attenuation levels reaching several decibels per kilometer during heavy precipitation [5]. This vulnerability necessitates meticulous network planning and robust fade margin design to ensure service availability, particularly for

*Corresponding Author

mission-critical applications and emerging technologies like autonomous vehicles and industrial automation [6].

The African continent presents unique challenges for 5G deployment due to its diverse climatic conditions and limited research on local propagation characteristics [7]. South Africa, as the continent's most industrialized economy, stands at the forefront of 5G adoption, yet comprehensive studies on rain attenuation specific to its urban environments remain conspicuously absent from the scientific literature [8]. Johannesburg, the nation's economic hub with a population exceeding 10 million, experiences a subtropical highland climate characterized by summer thunderstorms and moderate winter rainfall, creating an ideal testbed for investigating rain attenuation patterns in a developing urban context [9].

Previous research has predominantly focused on temperate regions or employed generalized models that may not accurately capture the nuanced rainfall patterns of Southern Africa [10]. The International Telecommunication Union (ITU) provides standardized attenuation models, but these require validation against local empirical data to ensure accuracy in specific geographical contexts [11]. Moreover, existing studies often overlook the temporal dimensions of rain attenuation, such as seasonal variations, diurnal cycles, and statistical distributions, that are crucial for designing adaptive networks capable of responding to dynamic environmental conditions [12].

This research addresses these gaps by conducting a comprehensive six-year analysis of rain attenuation characteristics in Johannesburg, focusing on both 5G Frequency Range 1 (FR1: 3.5 GHz) and Frequency Range 2 (FR2: 30 GHz). The study employs high-resolution hourly precipitation data from the South African Weather Service (SAWS) spanning 2010 to 2015, providing an unprecedented temporal resolution for attenuation analysis in the region. By integrating ITU-R models with advanced statistical techniques and time series analysis, this work aims to establish localized attenuation profiles that can inform evidence-based network planning decisions.

The primary objectives of this study are threefold: first, to quantify and compare rain attenuation for 5G FR1 and FR2 bands using established ITU-R models; second, to characterize the seasonal and diurnal patterns of attenuation to identify high-risk periods for network performance; and third, to perform comprehensive statistical analysis including distribution fitting, stationarity testing, and extreme value analysis to support robust fade margin design. The findings are expected to contribute practical guidelines for 5G deployment in Johannesburg and similar urban environments in developing regions, while advancing theoretical understanding of rain attenuation dynamics in subtropical climates.

2. Literature Review and Past Related Works

2.1. Attenuation due to Rain and its Models

The study of rain attenuation in wireless communications has evolved significantly since Ryde's pioneering work in the 1940s, which established the fundamental relationship between rainfall rate and signal degradation [13]. Modern attenuation prediction models can be broadly categorized into empirical, physical, and statistical approaches, each with distinct strengths and limitations [14]. Among these, the International Telecommunication Union's Radio Communication Sector (ITU-R) models have gained widespread acceptance as industry standards due to their balance of accuracy and computational simplicity [15, 16].

The ITU-R P.838-3 recommendation provides coefficients for calculating specific attenuation (dB/km) as a function of frequency (1-1000 GHz) and polarization, based on extensive global measurement campaigns [15]. This model,

derived from Mie scattering theory and validated against experimental data, assumes spherical raindrops following the Laws and Parsons distribution, an approximation that has proven reasonably accurate for temperate and tropical climates [17]. However, researchers have noted discrepancies in regions with atypical raindrop size distributions or intense convective rainfall, necessitating localized model adjustments [18].

Complementing the specific attenuation model, ITU-R P.530-18 addresses path attenuation by introducing effective path length reduction factors that account for rainfall inhomogeneity along the propagation path [16]. This approach recognizes that heavy rainfall is typically localized rather than uniform, a phenomenon particularly relevant to the convective thunderstorms common in Johannesburg's summer months [9]. Several studies have proposed modifications to these reduction factors for specific climates, including the Crane global model for North America and the EXCELL model for European conditions [19, 20].

2.2. Seasonal and Diurnal Variations in Rain Attenuation

Temporal variability in rainfall patterns significantly influences attenuation characteristics, yet this dimension has received comparatively limited attention in propagation literature [10]. Seasonal variations are particularly pronounced in regions with distinct wet and dry seasons, such as the monsoon climates of Asia and the summer rainfall regions of Southern Africa [12]. Studies in Nigeria by Ajayi and Ofoche (1984) [21] revealed attenuation peaks during the rainy season (April-October) that were 3-5 times higher than dry season values at 12 GHz. Similarly, research in India by Das *et al*. (2010) [10] documented seasonal attenuation variations exceeding 10 dB for Ku-band satellite links during monsoon months.

Diurnal cycles introduce additional complexity, with many regions exhibiting pronounced rainfall peaks during specific times of day. In tropical Africa, research by Nicholson (2018) [22] identified afternoon maxima in convective rainfall associated with daytime heating, while coastal regions often experience early morning peaks due to land-sea breeze interactions. For wireless network planning, these diurnal patterns are crucial as they may align with or contradict traffic load patterns, creating either compounded or offsetting effects on network performance [6].

The statistical characterization of rain attenuation has evolved from simple mean-value approaches to sophisticated distributional analyses incorporating higher-order moments [23]. Skewness and kurtosis metrics provide insights into the asymmetry and tail behavior of attenuation distributions, which are critical for designing fade margins that balance reliability against spectral efficiency [5]. Recent studies by Ojo *et al*. (2019) [18] in South Africa have applied extreme value theory to estimate return periods for severe attenuation events, providing valuable inputs for risk assessment in network planning.

3. Methodology

3.1. Research Location

Johannesburg (26°12′S, 28°02′E), situated on South Africa's Highveld plateau at approximately 1,750 meters above sea level, presents a unique propagation environment characterized by its subtropical highland climate (Köppen classification Cwb) [9]. The city experiences distinct seasonal patterns: summer (DJF: December-February) brings frequent afternoon thunderstorms with rainfall intensities occasionally exceeding 50 mm/h, autumn (MAM: March-May) features gradually decreasing rainfall, winter (JJA: June-August) is generally dry with occasional light precipitation, and spring (SON:

September-November) marks the transition to the rainy season with increasing convective activity [24].

3.2. Data Collection and Preprocessing

This study utilizes six years (January 2010-December 2015) of hourly precipitation data obtained from the South African Weather Service (SAWS), representing one of the most comprehensive atmospheric datasets available for Johannesburg. The recording station, located at OR Tambo International Airport (WMO ID: 683680), employs a tipping-bucket rain gauge with 0.1 mm resolution, maintained according to World Meteorological Organization standards [25].

Data preprocessing followed rigorous quality control protocols adapted from the methodology proposed by Yang et al. (2019) [26]. Missing values, constituting approximately 0.8% of the dataset, were imputed using temporal interpolation considering both diurnal and seasonal patterns. Suspect outliers, defined as values exceeding four standard deviations from the hourly mean for each month, underwent manual verification against neighboring stations when available. The final processed dataset comprises 52,584 hourly observations, each recording precipitation accumulation in millimeters.

Converting precipitation in mm to rain rate in mm/h is an important step that connects measured precipitation to attenuation. In this study, the collected hourly precipitation in mm is the same as the rain rate in mm/h for one hour integration time [11]. For contrast with investigations utilizing shorter integration times, Segal (1986) [27] established an approach which calculates one-minute rain rates.

3.3. Attenuation Calculation Framework

Rain attenuation calculations followed the ITU-R P.838-3 recommendation for specific attenuation [15] and ITU-R P.530-18 for path attenuation [16], with modifications to address local conditions. For attenuation calculations, the ITU-R model uses 1-minute integration time rain rate in mm/h. Since the available data in this work is hourly, the hourly precipitation in mm is equivalent to the rain rate in mm/h for that hour, therefore it is required to convert the hourly rain rate to 1-minute equivalent. However, for 1-minute integration time, the conversion can be done using [27]:

$$R_{1min} = R_{60min} * \left({}^{60}/_{T}\right)^{-\beta} \tag{1}$$

where R_{1min} represents the rain rate (mm/h) for a 1-minute integration time, R_{60min} denotes the hourly rain rate (mm/h), T is the integration time in minutes (60 for hourly data) such that $T = 60$ minutes (hourly) and β is a conversion factor (typically between 0.15 and 0.25), however, $\beta = 0.18$ as per Segal (1986) can be used [28].

The specific attenuation γ (dB/km) at frequency f (GHz) for vertical polarization was computed as [15]:

$$\gamma = k \times R^{\alpha} \tag{2}$$

where R represents rain rate (mm/h) for a 1-minute integration time, and k and α are frequency-dependent coefficients derived from ITU-R P.838-3 recommendation for frequencies from 1 to 1000 GHz. For this study, frequencies of 3.5 GHz (FR1) and 30 GHz (FR2) were selected as representative of current 5G network deployments, with coefficients $k = 0.000091$, $\alpha = 1.054$ for 3.5 GHz and $k = 0.167$, $\alpha = 1.000$ for 30 GHz [15].

Path attenuation A (dB) for a link distance d (km) incorporated the effective path length reduction factor r to account for rainfall spatial inhomogeneity [16]:

$$A = \gamma \times d \times r \tag{3}$$

where $r = 1/(1 + 0.045 \cdot d)$ represents the reduction factor for horizontal paths [16]. While this formulation assumes a default path length of *1 km* for comparative purposes, sensitivity analyses examined distances from *0.5* to *20 km* to capture typical urban cell sizes.

Therefore, the ITU-R P.530-18 rain attenuation prediction for 0.01% of the time is given by [16]:

$$A_{0.01} = \gamma_{0.01} \times L_{eff} \tag{4}$$

where $\gamma_{0.01}$ is the specific attenuation for the rain rate exceeded for 0.01% of the time ($R_{0.01}$), and L_{eff} is the effective path length given by $L_{eff} = r \times d$.

The attenuation exceeded for a percentage of time p (0.001% to 5%) can be calculated as [16]:

$$A_p = A_{0.01} \times \left(\frac{p}{0.01}\right)^{-(0.655+0.033\ln(p)-0.045\ln(A_{0.01})-\beta(1-p)\sin(\theta))} \tag{5}$$

where β is a coefficient that depends on frequency and θ is the path elevation angle (0 for terrestrial links).

The Cumulative Distribution Function (CDF) is given by [29]:

$$F(x) = P(X \leq x) \tag{6}$$

and the exceedance probability is [29]:

$$P(X > x) = 1 - F(x) \tag{7}$$

The peak rain rate distribution follows the modified Moupfouma (1987) model adapted for Southern African conditions [30]:

$$P(R > R_0) = \exp\left[-\left(\frac{R_0}{R_m}\right)^{\gamma}\right] \tag{8}$$

where $P(R > R_0)$ represents the probability that rain rate exceeds threshold R_0, R_m is the median rain rate for the location, and γ is a shape parameter characterizing rainfall intensity distribution [30]. This formulation enables estimation of exceedance probabilities critical for network availability calculations.

3.4. Framework for Statistical Analysis

The statistical analysis section of this study includes the descriptive statistics, trend and distribution analysis. This gives a perfect summary of the estimations of the rain attenuation over the specified location and period of study. The four seasons experienced in the study area are based on the typical climatological changes in South Africa, which are summer (DJF), autumn (MAM), winter (JJA), and spring (SON). The diurnal analysis gives the attenuation patterns for a period of 24 hours, which offers a specific consideration to peak periods that might match with network traffic loads.

4. Results and Discussion

This section presents and discusses the results obtained from the analysis of precipitation and rain-induced signal attenuation in Johannesburg over the period 2010–

2015. The findings are integrated to provide a comprehensive understanding of the statistical characteristics, temporal variations, and comparative performance of the studied frequency bands.

4.1. Statistical Analysis of Precipitation and Attenuation

The foundational descriptive statistics for precipitation, rain rate, and specific/path attenuation at 3.5 GHz and 30 GHz are summarized in Table 1. The dataset comprises 52,584 hourly samples, indicating a robust temporal coverage. A key observation is the high frequency of zero-rainfall events, as evidenced by the median, first quartile (Q1), third quartile (Q3), and 95th percentile values being zero for all parameters. This results in an Interquartile Range (IQR) of zero, confirming that over 75% of the observed period was dry.

The mean path attenuations are very low (7.44×10^{-6} dB at 3.5 GHz and 0.0126 dB at 30 GHz), reflecting the overall low-rainfall climate of Johannesburg. However, the maximum values reveal the potential for significant signal degradation during extreme events, reaching 0.0045 dB and 6.74 dB for the 3.5 GHz and 30 GHz bands, respectively. The Coefficient of Variation (CV) exceeds 980% for all series, indicating extremely high variability relative to the mean, which is characteristic of intermittent, event-driven phenomena like rainfall.

The calculated skewness and kurtosis values are exceptionally high (Skewness > 20, Kurtosis > 630). A skewness value significantly greater than zero indicates a highly right-skewed (positively skewed) distribution. This means the vast majority of data points are clustered near zero (no rain/no attenuation), with a long tail extending towards high-value extreme events. The extraordinarily high kurtosis (leptokurtic distribution) signifies that these extreme events in the tail are more frequent and severe than would be expected in a normal distribution. Together, these metrics quantitatively confirm that the distributions of precipitation and attenuation are non-Gaussian and heavily dominated by a preponderance of zero values punctuated by rare but intense rain events. This has critical implications for modeling and system design, as average values are not representative, and systems must be engineered to handle these extremes.

Table 1. Comprehensive descriptive statistics for precipitation and attenuation

Metrics	Precipitation (mm)	Rain Rate (mm/h)	Specific Attenuation 3.5 GHz (dB/km)	Specific Attenuation 30 GHz (dB/km)	Path Attenuation 3.5 GHz (dB)	Path Attenuation 30 GHz (dB)
Count	52584	52584	52584	52584	52584	52584
Mean	0.0788	0.0788	7.78E-06	0.0132	7.44E-06	0.0126
Median	0	0	0	0	0	0
Std	0.7733	0.7733	8.07E-05	0.1291	7.72E-05	0.1236
Min	0	0	0	0	0	0
Max	42.2	42.2	0.0047	7.0474	0.004498	6.743923
Variance	0.5979	0.5979	6.51E-09	0.0167	5.96E-09	0.0153
CV	981.8263	981.8263	1037.739	981.8263	1037.739	981.8263
IQR	0	0	0	0	0	0
Skewness	20.6655	20.6655	22.4714	20.6655	22.4714	20.6655
Kurtosis	630.036	630.036	746.716	630.036	746.716	630.036
Q1	0	0	0	0	0	0
Q3	0	0	0	0	0	0
95th_percentile	0	0	0	0	0	0
99th_percentile	2.2	2.2	0.0002	0.3674	0.0002	0.3516

The heatmap in Figure 1 provides a visual synthesis of these statistics, allowing for quick comparison of central tendency, dispersion, and extreme values across all measured variables, reinforcing the dominance of dry conditions and the high-impact nature of wet events.

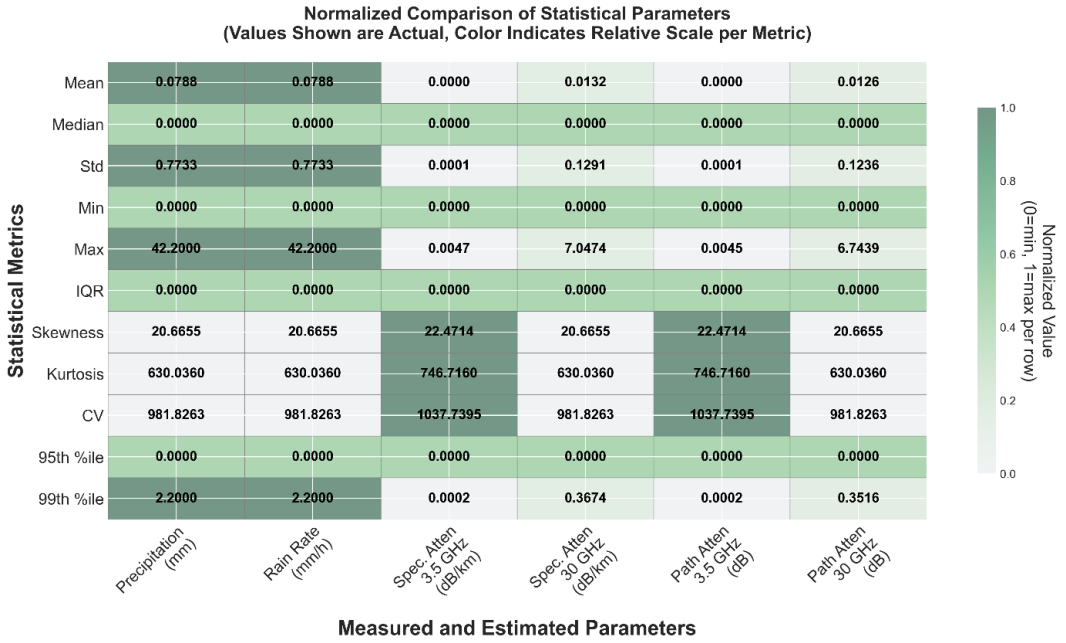

Figure 1. Heatmap showing the overall statistics for precipitation, rain rate and rain attenuation for Johannesburg across 2010 to 2015

4.2. Precipitation Trend and Variations

Figure 2 illustrates the overall temporal variation and occurrence of precipitation from 2010 to 2015. The histogram and box plots in Figures 2(a) and 2(b) show the distribution of precipitation, with distributions heavily concentrated at zero, and progressively dipping as the distributions tends to move away from zero. The Cumulative Distribution Functions (CDFs) in Figure 2(c) is relevant for predicting the rain rate and attenuation. It shows that for 99% of the time, the precipitation is below 2.2 mm. The plot in Figure 2(d) reveals the episodic nature of rainfall in Johannesburg, with distinct wet and dry periods. The concentration of precipitation events during specific months aligns with the known summer rainfall pattern of the region, setting the context for the observed attenuation patterns discussed in subsequent sections. Figure 2(e) shows the various annual precipitations across the entire period under study. The inter-annual variability is observable, with certain years experiencing more frequent or intense rainfall events. The rain rate distribution is presented in Figure 2(f), with distributions heavily concentrated at zero mm/h.

4.3. Variations of Rain Attenuation

A detailed analysis of rain attenuation at both frequency bands over path length of 1 km is presented in Figure 3. Subplots (a) and (b) show the distribution of attenuation at 3.5 GHz (FR1) and 30 GHz (FR2), respectively. The histograms visually echo the statistical findings from Section 4.1, with distributions heavily concentrated at zero. Subplot (c) directly compares these distributions on a logarithmic scale, clearly demonstrating that attenuation at 30 GHz is orders of magnitude higher than at 3.5 GHz for the same rain conditions.

The relationship between rain rate and attenuation is shown in Subplot (d). As expected from theoretical models (e.g., ITU-R P.838), attenuation increases with rain rate, and the slope is markedly steeper for the higher frequency (30 GHz). The CDFs in Subplots (e) and (f) are crucial for link budget design. They show that for 99% of the time, attenuation is below 0.0002 dB at 3.5 GHz and below 0.35 dB at 30 GHz. However, to cater for the most extreme 0.01% of events (99.99% availability), systems must handle up to the maximum values recorded.

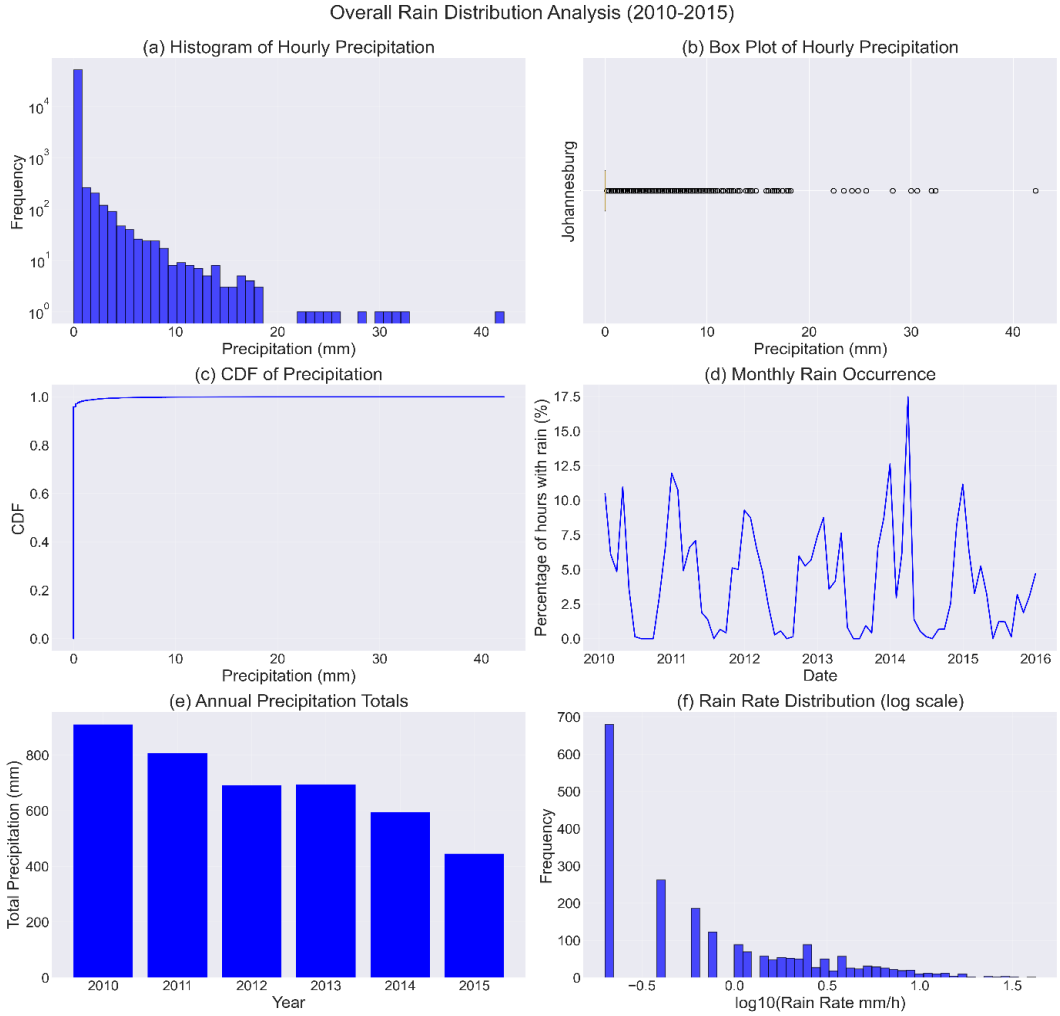

Figure 2. Overall precipitation variation and occurrence for Johannesburg across 2010 to 2015

4.4. Seasonal Analysis

The strong seasonal dependence of rainfall in Johannesburg profoundly impacts signal attenuation. Figures 4(a) and 4(b) provide a visual breakdown of seasonal precipitation and attenuation by season for both frequencies, respectively. The results confirm that the highest average precipitation and attenuation occur during the summer months of December, January, and February (DJF), followed by the spring (SON) and autumn (MAM) seasons. The winter months (JJA) contribute minimally to annual precipitation and attenuation.

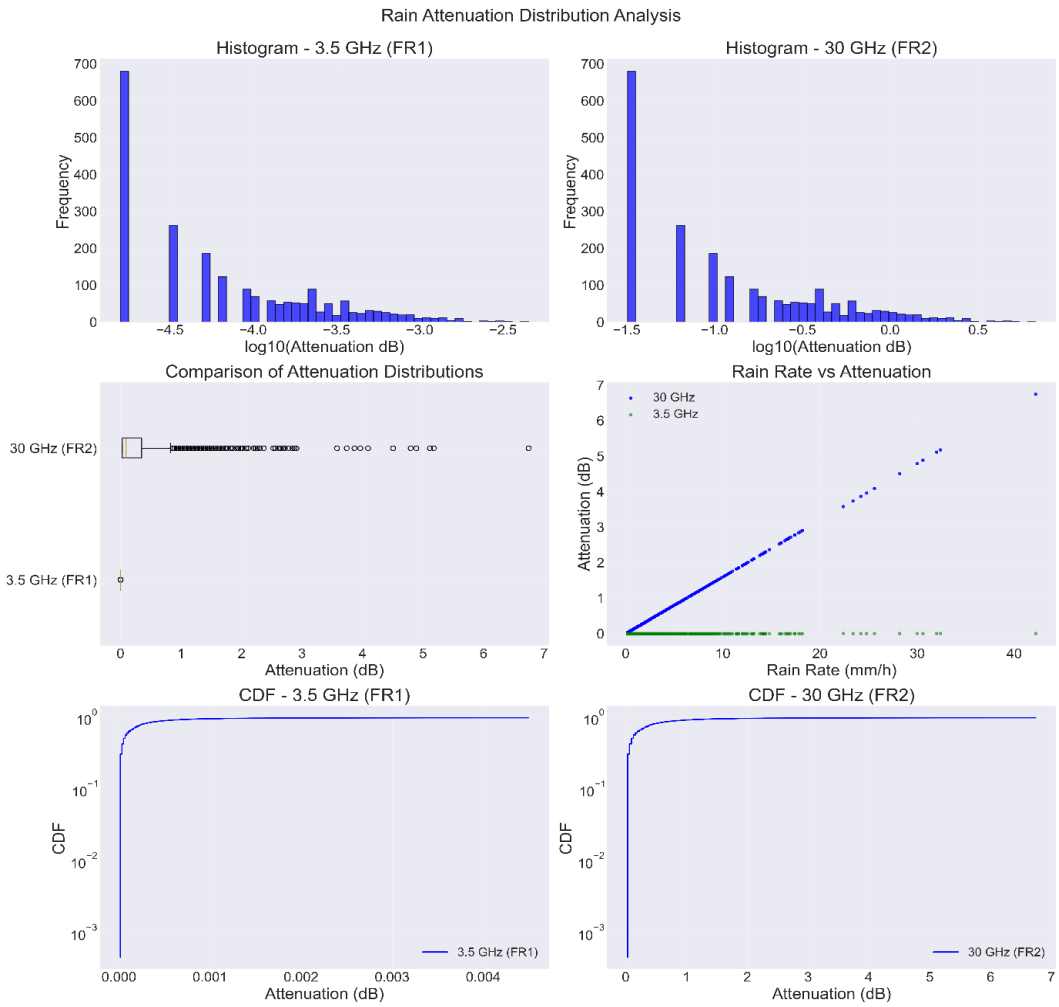

Figure 3. Rain attenuation analysis plots for Johannesburg at 3.5 GHz and 30 GHz across 2010 to 2015 (a) Rain attenuation distribution at 3.5 GHz (FR1); (b) Rain attenuation distribution at 30 GHz (FR2); (c) Comparison of attenuation distributions; (d) Rain rate vs attenuation at 3.5 GHz (FR1) and 30 GHz (FR2); (e) CDF of attenuation at 3.5 GHz (FR1); and (f) CDF of attenuation at 30 GHz (FR2).

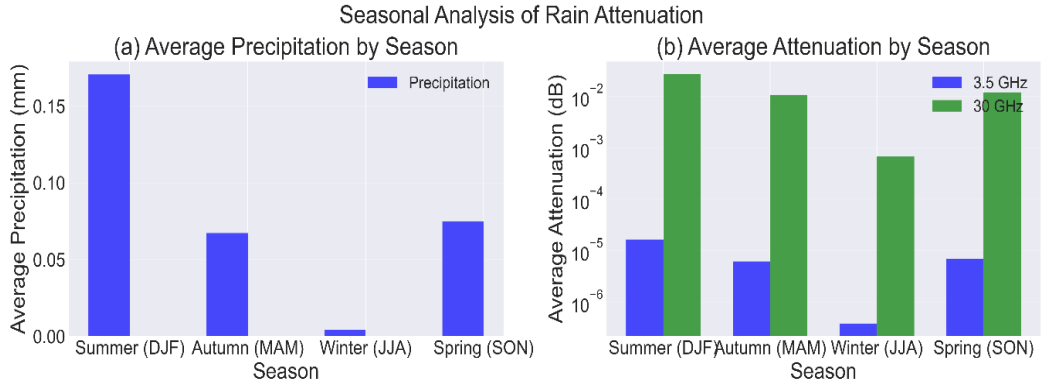

Figure 4. Seasonal analysis of rain attenuation for Johannesburg at 3.5 GHz and 30 GHz across 2010 to 2015

This seasonal trend is quantified in Tables 2 and 3, which present the maximum seasonal attenuation at different path lengths (1, 3, 5, and 7 km) for 3.5 GHz and 30 GHz, respectively. The graphical comparisons in Figures 5 and 6 effectively illustrate the compounded effect of season and path distance on maximum attenuation, emphasizing the

need for seasonal fade margins in system design, particularly for high-frequency applications.

Table 2. Comparison of seasonal rain attenuation at 3.5 GHz based on distance

Season	Rain %	1 km	3 km	5 km	7 km
		Maximum Attenuation (dB)			
DJF	7.62	0.0045	0.0124	0.0192	0.0250
MAM	4.60	0.0024	0.0067	0.0103	0.0134
JJA	0.40	0.0008	0.0021	0.0032	0.0042
SON	4.03	0.0034	0.0094	0.0145	0.0189

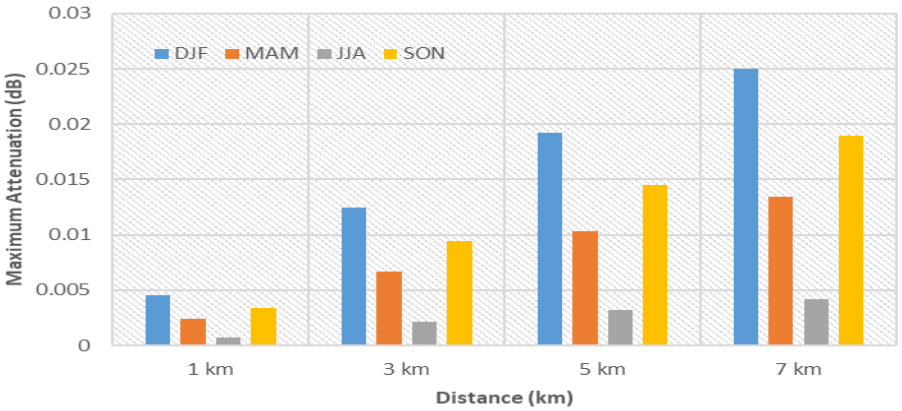

Figure 5. Comparison of maximum rain attenuation at 3.5 GHz based on season and distance for Johannesburg across 2010 -2015

Table 3. Comparison of seasonal rain attenuation at 30 GHz based on distance

Season	Rain %	1 km	3 km	5 km	7 km
		Maximum Attenuation (dB)			
DJF	7.62	6.7439	18.6275	28.7649	37.5147
MAM	4.60	3.7395	10.3290	15.9502	20.8020
JJA	0.40	1.2465	3.4430	5.3167	6.9340
SON	4.03	5.1778	14.3017	22.0849	28.8027

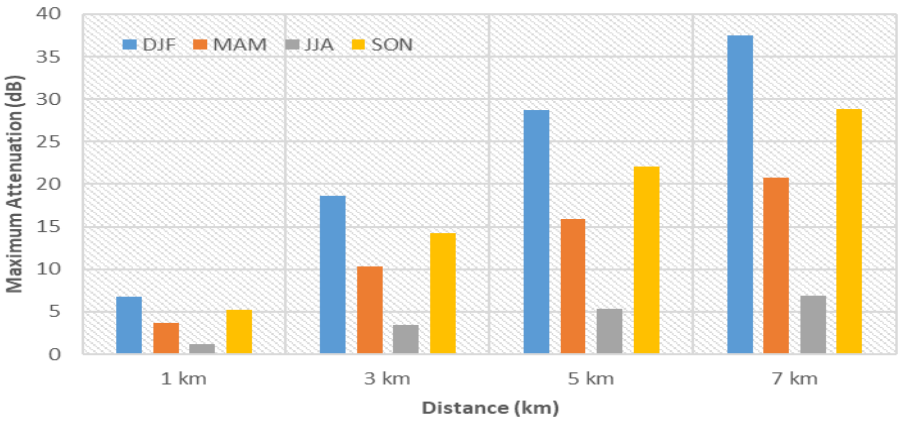

Figure 6. Comparison of maximum rain attenuation at 30 GHz based on season and distance for Johannesburg across 2010 -2015

Tables 2 and 3 also include the percentage of total rainfall contributed by each season ("Rain %"). A direct correlation is observed between the seasonal rain percentage and the maximum attenuation. At 3.5 GHz (Table 2 and Figure 5), maximum attenuation is low across all seasons, with DJF values reaching 0.025 dB for a 7 km path. The values scale approximately linearly with distance. At 30 GHz (Table 3 and Figure 6), attenuation is severe across all seasons. During DJF, a 7 km path can experience attenuation exceeding 37.5 dB. This highlights the critical vulnerability of higher-frequency links (e.g., for 5G FR2 or satellite Ka-band) to seasonal summer storms.

4.5. Monthly Variations

A finer temporal resolution is provided by the monthly analysis. Figure 7(a) shows the monthly variation of average attenuation over 1 km link distance, clearly identifying November through February as the period of highest risk. The peak monthly average attenuation at 30 GHz is nearly an order of magnitude higher than the annual average, underscoring the concentration of impactful events. Figure 7(b) reveals higher standard deviation for the periods of higher risk, and Figure 7(c) indicates that these months have higher maximum attenuations compared to the other months. This coincides to what have been earlier discussed that the summer and spring months have higher attenuation than the months of other seasons.

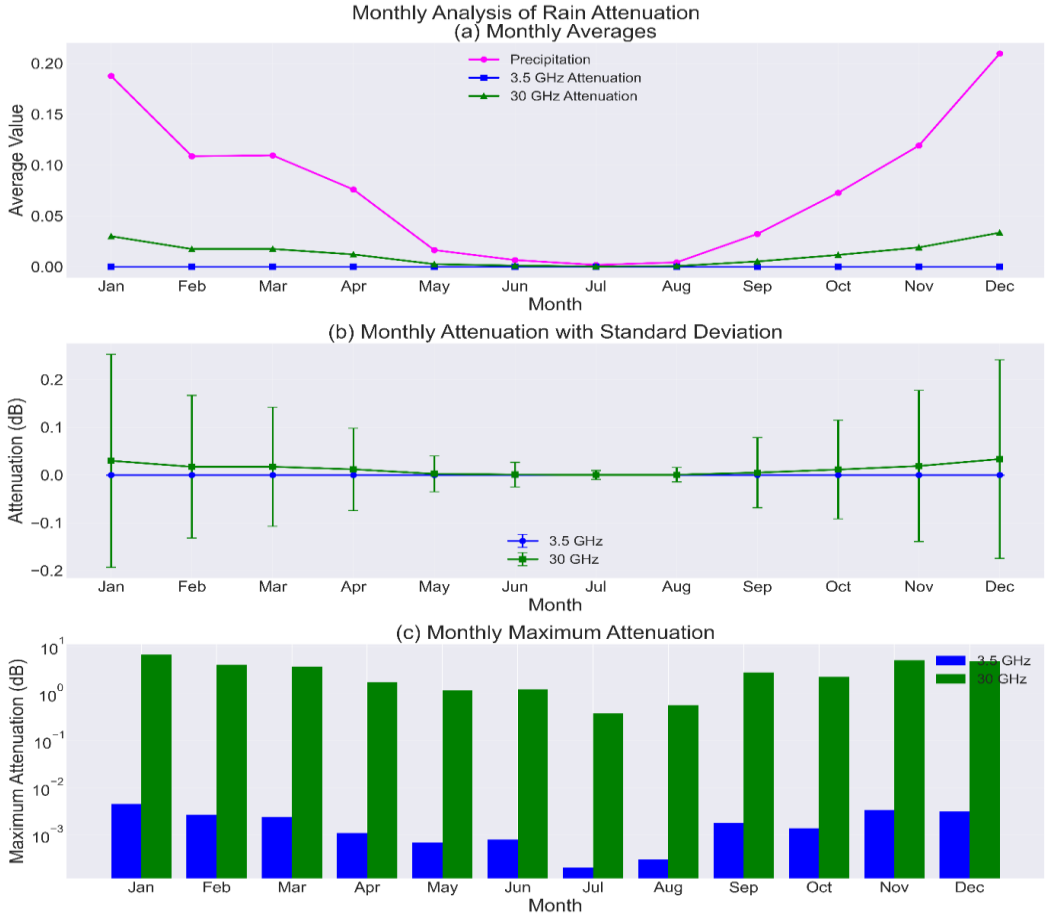

Figure 7. Monthly variation of average attenuation at 3.5 GHz and 30 GHz for Johannesburg across 2010 to 2015.

Figure 8 presents heatmaps of hourly vs. monthly attenuation for both 3.5 GHz and 30 GHz. These plots reveal not only which months are worst but also what time of day attenuation is most likely. The heatmaps suggest a propensity for high-attenuation events during the afternoon and early evening hours in the peak summer months, likely

associated with convective thunderstorms typical of the region. This diurnal pattern within high-risk months is crucial for planning maintenance or scheduling critical communications.

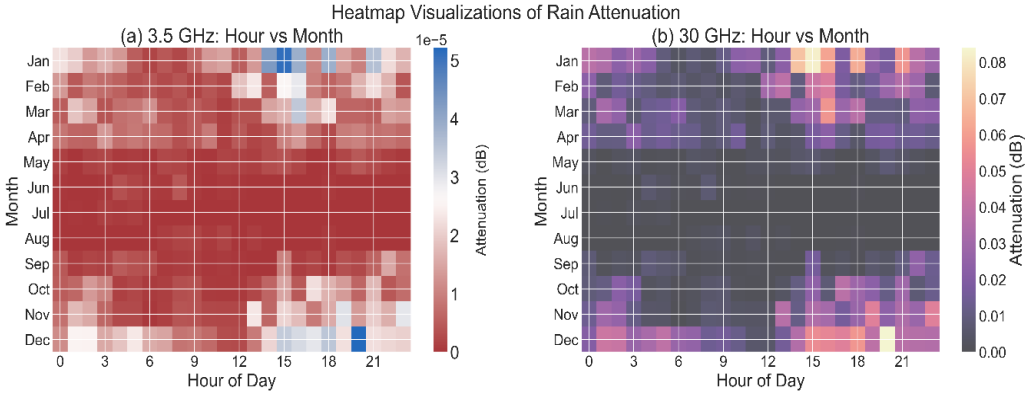

Figure 8. Heatmap of hourly vs monthly rain attenuation over a link distance of 1 km at (a) 3.5 GHz and (b) 30 GHz (FR2)

4.6. Diurnal Variations of Rain Attenuation

The diurnal cycle is explicitly analyzed in Figure 9. The plots show a pronounced peak in attenuation during the late afternoon to early night period (approximately 15:00 to 21:00 local time), as can be clearly seen in Figure 9(a). This period also experiences high standard deviation values as seen in Figure 9(b). Figure 9(c) shows hourly rain incidence probability, where the early night period also shows higher percentage of hours with rain. The maximum attenuation by hour plot shown in Figure 9(d) reveals that the maximum attenuation of approximately 7 dB and 0.005 dB at 30 GHz and 3.5 GHz respectively, were observed at 16:00 hours local time. This pattern is consistent across both frequencies and aligns with the climatology of convective rainfall in interior regions of South Africa, which is often driven by daytime heating. Understanding this diurnal cycle allows network operators to anticipate periods of high fade probability and implement dynamic link adaptation strategies.

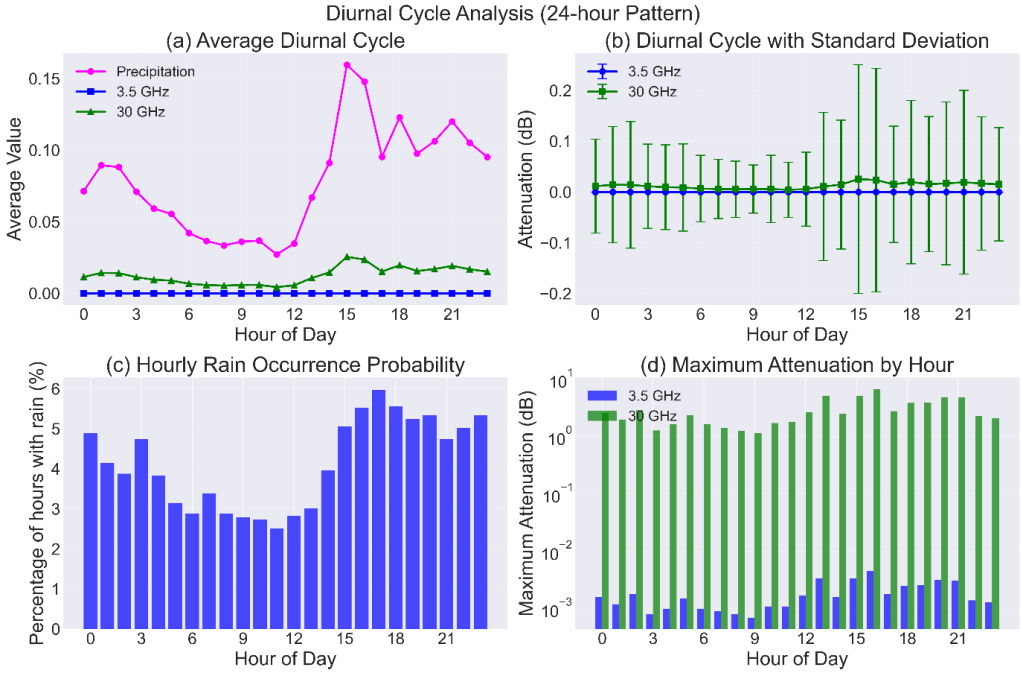

Figure 9. Diurnal variation plots of rain attenuation at 3.5 GHz and 30 GHz over 1 km link distance for Johannesburg across 2010 to 2015.

4.7. Daily Time Series Trend of Rain Attenuation

The daily evolution of rain rate and attenuation throughout a representative year (2010) is depicted in Figure 10. This time-series visualization captures the sporadic nature of rain events. It clearly shows how attenuation over 1 km at 30 GHz (FR2) spikes dramatically during rainfall events, while the response at 3.5 GHz (FR1) is barely perceptible on the same scale. The plot reinforces the concept that the high-frequency link is significantly more sensitive to the prevailing meteorological conditions and experiences much deeper fades over shorter durations.

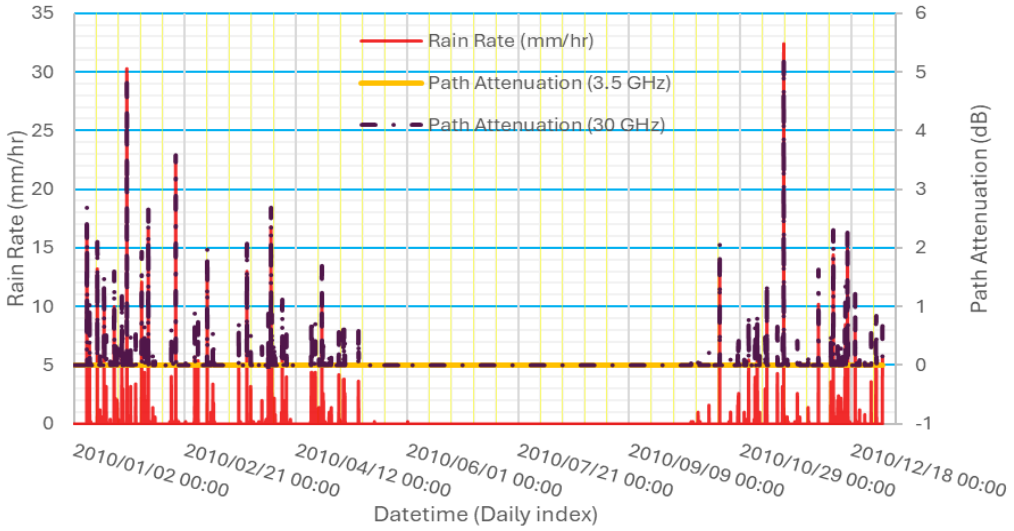

Figure 10. Daily time series for rain rate and attenuation over 1 km link distance at 3.5 GHz and 30 GHz for Johannesburg across year 2010

4.8. Comparison between the Selected Frequency Bands

A direct quantitative comparison between the 3.5 GHz (FR1) and 30 GHz (FR2) bands over 1 km link distance is consolidated in Table 4. The key metrics underscore the vastly different propagation environments:

- **Magnitude of Attenuation:** The mean and maximum attenuation at 30 GHz are approximately 1,600 to 1,750 times greater than at 3.5 GHz. This immense ratio is the most salient finding for network planning.
- **Impact on Availability:** While attenuation exceeding 1 dB is virtually non-existent at 3.5 GHz (0% probability), it occurs for about 0.28% of the time (≈25 hours per year) at 30 GHz. Similarly, severe fades >5 dB have a probability of 0.0057% (≈5 hours per year) at 30 GHz.
- **Design Implications:** For a terrestrial 5G network, these results strongly advocate for the use of the 3.5 GHz band (FR1) for wide-area coverage and reliability, given its robustness to rain fade. The 30 GHz band (FR2) offers high capacity but requires very short cell ranges (small cells) and sophisticated fade mitigation techniques (e.g., beamforming, diversity, adaptive modulation and coding) to maintain link availability during the summer rainy season. For satellite communications in the Ka-band, these results confirm the necessity of substantial fade margins for services targeting the Johannesburg region.

Table 4. Comparison statistics between FR1 (3.5 GHz) and FR2 (30 GHz)

Metric	3.5 GHz	30 GHz	Ratio (30/3.5)
Mean Attenuation (dB)	7.44E-06	0.0126	1691.63
Median Attenuation (dB)	0	0	NaN
Std Deviation (dB)	7.72E-05	0.1236	1600.48
Maximum Attenuation (dB)	0.0045	6.7439	1499.37
95th Percentile (dB)	0	0	NaN
99th Percentile (dB)	0.0002	0.3516	1758.67
Probability of Attenuation > 1 dB (%)	0	0.2815	NaN
Probability of Attenuation > 5 dB (%)	0	0.0057	NaN
Probability of Attenuation > 10 dB (%)	0	0	NaN

In conclusion, the integrated results and discussion confirm that rain-induced attenuation is a highly variable, seasonal, and diurnally influenced phenomenon in Johannesburg. The impact is dramatically more severe at 30 GHz compared to 3.5 GHz. Effective design and planning of wireless communication systems, especially those leveraging higher frequency bands for 5G and beyond, must account for these statistical characteristics, temporal patterns, and extreme event probabilities to ensure desired service quality and availability.

5. Conclusion

This study has conducted a detailed investigation into the characteristics of rain-induced attenuation for potential 5G communication links in Johannesburg, South Africa, over a six-year period. The analysis of 3.5 GHz (FR1) and 30 GHz (FR2) bands, grounded in ITU-R propagation models and high-resolution meteorological data, yields several critical insights for network planning and deployment.

The most salient finding is the dramatic difference in attenuation magnitude between the two frequency bands. The 30 GHz band experiences attenuation that is orders of magnitude higher than the 3.5 GHz band, with a mean ratio exceeding 1,600:1. While the 3.5 GHz link remains largely unaffected by rain, the 30 GHz link suffers significant degradation, with a non-zero probability (0.28%) of attenuation exceeding 1 dB and maximum values reaching nearly 38 dB for longer paths during extreme summer storms. This stark contrast strongly advocates for a strategic, hybrid network deployment: utilizing the robust, lower-frequency FR1 band for wide-area coverage and reliability, while deploying the high-capacity FR2 band selectively in ultra-dense small-cell configurations with sophisticated fade mitigation techniques.

The temporal analysis revealed that rain attenuation is not a static threat but a highly dynamic one. The strong seasonal dependency, with peak attenuation concentrated in the summer and spring months, necessitates the application of seasonal fade margins in link budgets. Furthermore, the identified diurnal peak in attenuation during the late afternoon and early evening hours, coinciding with convective thunderstorm activity, provides a crucial window for proactive network management. Understanding these patterns allows operators to anticipate periods of high vulnerability and implement dynamic resource allocation or adaptive coding and modulation schemes.

Statistically, the distributions of both precipitation and attenuation were confirmed to be highly non-Gaussian, characterized by extreme positive skewness and kurtosis. This confirms that system design based on average values is inadequate; engineering must focus on mitigating the impact of rare but severe

extreme events to guarantee high availability. The comprehensive statistics and probability of exceedance data provided in this work serve as a valuable localized reference for calculating realistic fade margins.

In conclusion, this research provides empirically derived, location-specific propagation knowledge that is currently scarce for African urban environments. The findings highlight the compounded challenges of deploying high-frequency 5G networks in subtropical climates and offer practical guidelines for ensuring service reliability. Future work should focus on validating these model-based results with actual measured attenuation data from operational 5G links and extending the analysis to other major cities across Southern Africa's diverse climatic zones.

Acknowledgments

The authors wish to thank Tshwane University of Technology, Pretoria for the support provided during the course of this study.

REFERENCES

[1] *J. G. Andrews, S. Buzzi, W. Choi, S. V. Hanly, A. Lozano, A. C. Soong and J. C. Zhang, "What will 5G be?", IEEE Journal on Selected Areas in Communications, vol. 32, no. 6, (2014), pp. 1065-1082. doi:10.1109/JSAC.2014.2328098.*

[2] *T. S. Rappaport, S. Sun, R. Mayzus, H. Zhao, Y. Azar, K. Wang, G. N. Wong, J. K. Schulz, M. Samimi and F. Gutierrez, "Millimeter wave mobile communications for 5G cellular: It will work!", IEEE Access, vol. 1, (2013), pp. 335-349. doi:10.1109/ACCESS.2013.2260813.*

[3] *F. Moupfouma and E. M. Martins, "Handbook of Research on Wireless Communications and Networks", IGI Global, (2015).*

[4] *R. L. Olsen, D. V. Rogers and D. B. Hodge, "The aR^b relation in the calculation of rain attenuation", IEEE Transactions on Antennas and Propagation, vol. 26, no. 2, (1978), pp. 318-329. doi:10.1109/TAP.1978.1141845.*

[5] *A. Ghasemi, A. Abedi and F. Ghasemi, "Propagation Engineering in Wireless Communications", Springer International Publishing, (2017).*

[6] *M. Cheffena, "Propagation channel characteristics of industrial wireless sensor networks", IEEE Antennas and Propagation Magazine, vol. 58, no. 1, (2016), pp. 66-73. doi:10.1109/MAP.2016.2520235.*

[7] *J. S. Ojo, M. O. Ajewole and L. D. Emiliani, "Rain rate and rain attenuation prediction for satellite communication in Ku and Ka bands over Nigeria", Progress in Electromagnetics Research B, vol. 5, (2018), pp. 207-223.*

[8] *N. O. Oyie and T. J. Afullo, "Rainfall rate modeling for microwave propagation in South Africa", Progress in Electromagnetics Research M, vol. 58, (2017), pp. 55-67. doi:10.2528/PIERM17031303.*

[9] *C. L. Müller, L. Chapman, S. Johnston, C. Kidd, S. Illingworth, G. Foody, A. Overeem and T. Wagner, "Crowdsourcing for climate and atmospheric sciences: current status and future potential", International Journal of Climatology, vol. 34, no. 12, (2014), pp. 3185-3203. doi:10.1002/joc.3910.*

[10] *S. Das, A. Maitra and A. K. Shukla, "Rain attenuation modeling in the 10–100 GHz frequency using drop size distributions for different climatic zones in tropical India", Progress in Electromagnetics Research B, vol. 25, (2010), pp. 211-224. doi:10.2528/PIERB10040705.*

[11] *ITU-R, "Characteristics of precipitation for propagation modelling (Recommendation P.837-7)", International Telecommunication Union, (2017).*

[12] *A. T. Adediji and M. O. Ajewole, "Vertical profile of rain rate and rain attenuation for satellite communication in tropical and subtropical regions of Africa", Radio Science, vol. 43, no. 4, (2008), pp. RS4008. doi:10.1029/2007RS003775.*

[13] *J. W. Ryde, "The attenuation and radar echoes produced at centimetre wavelengths by various meteorological phenomena", Meteorological Factors in Radio-Wave Propagation, (1946), pp. 169-188.*

[14] *F. Moupfouma, "Improvement of rain attenuation prediction methods for terrestrial microwave links", Annales des Télécommunications, vol. 64, no. 11-12, (2009), pp. 801-812. doi:10.1007/s12243-009-0107-0.*

[15] *ITU-R, "Specific attenuation model for rain for use in prediction methods (Recommendation P.838-3)", International Telecommunication Union, (2005).*

[16] *ITU-R, "Propagation data and prediction methods required for the design of terrestrial line-of-sight systems (Recommendation P.530-18)", International Telecommunication Union, (2021).*

[17] *G. O. Ajayi, S. Feng, S. M. Radicella and B. M. Reddy, "Handbook on Radio Propagation Related to Satellite Communications in Tropical and Subtropical Countries", The Abdus Salam International Centre for Theoretical Physics, Trieste, (1996).*

[18] *J. S. Ojo, P. A. Owolawi and M. M. Mphahlele, "Seasonal variation of rain attenuation based on drop size distributions for temperate continental climate", Journal of Atmospheric and Solar-Terrestrial Physics, vol. 193, (2019), pp. 105067. doi:10.1016/j.jastp.2019.105067.*

[19] *R. K. Crane, "Prediction of attenuation by rain", IEEE Transactions on Communications, vol. 28, no. 9, (1980), pp. 1717-1733. doi:10.1109/TCOM.1980.1094844.*

[20] *O. Fišer, V. Brázda and V. Bárták, "EXCELL rain attenuation model adapted to Canadian climate", Radioengineering, vol. 13, no. 4, (2004), pp. 35-39.*

[21] *G. O. Ajayi and E. B. Ofoche, "Some tropical rainfall rate characteristics at Ile-Ife for microwave and millimeter wave applications", Journal of Climate and Applied Meteorology, vol. 23, no. 4, (1984), pp. 562-567. doi:10.1175/1520-0450(1984)023<0562:STRRCA>2.0.CO;2.*

[22] *S. E. Nicholson, "The ITCZ and the seasonal cycle over equatorial Africa", Bulletin of the American Meteorological Society, vol. 99, no. 2, (2018), pp. 337-348. doi:10.1175/BAMS-D-16-0287.1.*

[23] *J. S. Mandeep, S. I. S. Hassan and M. F. Ain, "Rain attenuation predictions at Ku-band in South East Asia countries", Progress in Electromagnetics Research, vol. 76, (2007), pp. 65-74. doi:10.2528/PIER07061204.*

[24] *P. D. Tyson and R. A. Preston-Whyte, "The Weather and Climate of Southern Africa", Oxford University Press, (2000).*

[25] *WMO, "Guide to Meteorological Instruments and Methods of Observation (8th ed.)", World Meteorological Organization, (2018).*

[26] *S. Yang, J. Liu, Y. Wang and Y. Liu, "Quality control of hourly precipitation data from automatic weather stations in China", Journal of Applied Meteorology and Climatology, vol. 58, no. 7, (2019), pp. 1487-1496. doi:10.1175/JAMC-D-18-0264.1.*

[27] *B. Segal, "The influence of rain gauge integration time on measured rainfall-intensity distribution functions", Journal of Atmospheric and Oceanic Technology, vol. 3, no. 4, (1986), pp. 662-671. doi:10.1175/1520-0426(1986)003<0662:TIORGI>2.0.CO;2.*

[28] *J. Määtänen, L. Lamberg and M. Koivisto, "Time scaling of rainfall rate statistics for microwave link planning", Proceedings of the IEEE International Symposium on Personal, Indoor and Mobile Radio Communications, (2014), September 2-5.*

[29] *O. A. Layioye, "The Impact of Visibility Range and Atmospheric Turbulence on Free Space Optical Link Performance in South Africa", Doctoral dissertation, University of KwaZulu-Natal, South Africa (2022). Available: https://researchspace.ukzn.ac.za/handle/10413/21828.*

[30] *F. Moupfouma, "Rainfall rate distribution for radio system design", Proceedings of the IEEE, vol. 75, no. 4, (1987), pp. 524-525. doi:10.1109/PROC.1987.13757.*